Design and Implementation of a Kalman Filter-Based Time-Varying Harmonics Analyzer

S. H. Hosseini **K. Mohammadi**

Electrical Engineering Department

Sharif University of Technology

Tehran, Iran

Abstract: Nowadays with increasing use of numerous nonlinear loads, voltage and current harmonics in power systems are one of the most important problems power engineers encounter. Many of these nonlinear loads, because of their dynamic natures, inject time-varying harmonics into power system. Common techniques applied for harmonics measurement and assessment such as FFT have significant errors in present of time-varying harmonics due to the time-windows applied. In this paper, a Kalman filter-based algorithm is developed and implemented for measuring time-varying harmonics. The efficiency of the proposed algorithm has been successfully tested in off-line mode by various computer simulations. Based on this algorithm, a prototype harmonic analyzer has been designed, fabricated and used for on-line harmonic monitoring and assessment studies. To assess the severity of time-varying harmonics, cumulative time indices that are computed in real-time using the output of the analyzer are proposed. In addition, new cumulative time curves for total harmonic distortion and individual harmonic distortions are presented. Also, an auto-synchronization algorithm is proposed to accompany the Kalman filter algorithm in order to eliminate the errors occurred due to the variations in the incoming signal frequency.

Keywords:Time-Varying harmonics, Kalman filter, Power quality, Fast Fourier transform.

1. INTRODUCTION

The widespread development of power electronics devices and application of nonlinear loads, have increased the harmonic distortion in power system voltage and current waveforms. Thus, the conventional methods used for measuring and assessment of power system electrical parameters are not qualified anymore. In addition to the higher level of distortion in voltage and current waveforms, the new nonlinear loads have also changed the nature of the distortion. As an example, good number of motors used in industry have start-stop cycles and therefore the motor speed controller has to change its working

[Downloaded from jiaeee.com on 2026-11-20]

point periodically, the result of which is the time-varying harmonics injected into the system [1].

Accurate measurement of power system harmonics is essential in order to evaluate harmonic distortion in both current and voltage waveforms. Several methods have been applied for harmonics measurement such as, multi filter analyzers, frequency sweepers, quadratic transformers and different forms of Fourier transform among which the fast Fourier transform (FFT) is the most common approach applied in harmonic analyzer equipments [2-5]. When FFT is used, time windowing must be considered for the real-time signals to obtain two-dimensional spectra in time-frequency plane. Some drawbacks arise because of this time windowing. These drawbacks are even severer in present of time-varying harmonics. Theoretically, fast Fourier transform will be accurate only if the following assumptions can be made:

1-Waveform is periodic and stationary

2- Sampling frequency is greater than twice of the highest frequency in the signal

3- Number of periods in each time window is an integer and

4- Each frequency in the signal is an integer multiple of the frequency resolution dictated by the time window.

When these assumptions are satisfied, the result of FFT is accurate. But in many cases, even in absence of time-varying harmonics, they are not satisfied [6-8]. For example, the sampling frequency usually is constant but the power system fundamental frequency has deviations from the nominal value. Thus, the third assumption is not justified. This leads to an effect called "spectral leakage" [9]. In this case, for a pure sinusoidal waveform with 1% frequency deviation, the FFT measures a total harmonic distortion of 5%. As another example, in absence of the fourth assumption, the "picket-fence" effect occurs that leads to errors in the characteristic harmonics measurement. This effect, in both cases of stationary signals with fundamental frequency deviation and signals with time-varying harmonics can occur.

The above four assumptions often can't be satisfied for time-varying signals, therefore the analysis of these signals by means of Fourier transform in many cases leads to significant errors. Regardless of those assumptions, Fourier transform is not suitable for time-frequency studies because of the time-resolution and frequency-resolution trade off, i.e. decreasing time window size improves the time resolution but frequency resolution is decreased and vise versa. In other words, all harmonic orders have to be studied under a common time resolution in FFT, contradicting the requirement that higher order harmonics must be presented in higher time resolutions.

Many attempts have been made to apply different measurement methods with the ability of time-varying harmonics tracking such as, using group energy concept with FFT [6], applying non-square time windows in FFT implementation [7], applying artificial neural networks for harmonic tracking [10, 11] and, applying wavelet transform for harmonic measurement [12, 13]. Each of these methods has been successful in some cases but still some problems exist with applying them in practice. For example, very high computational requirements for wavelet based methods, limited application of neural network based methods in different harmonic patterns and, lack of proper operation of FFT based methods when encountering fast changing harmonics are of the main problems.

The challenges of the multimode RF front-end design are set by the standards and are related to different reception bands as shown in Table 1. The GSM operates at 900 MHz, the DCS operates at 1800 MHz, and the WCDMA operates at 2100 MHz. In addition, these systems have different channel spacing and symbol rates. In the past, multimode receivers have been realized as a multiple number of single-mode receivers thus occupying a large area and being rather costly. A direct conversion receiver (DCR) is considered as feasible architecture for multimode mobile wireless applications [1]-[9]. A DCR is amenable to monolithic integration, provides

2. Kalman Filter-Based Time-Varying Harmonics Measurment Algorithm

The state variable representations of signals including harmonics suitable for Kalman filter-based approach are well described in [14-16]. In this section, the derivation of equations for Kalman filter algorithm (KFA) for signals including time-varying harmonics is briefly stated.

Consider a sinusoidal signal with frequency ω, phase angle θ and amplitude $A(t)$, where $A(t)$ represents a combination of a constant value plus a time-varying component. This noise free signal may be expressed as:

$$s(t) = A(t)\cos(\omega t + \theta) = A(t)\cos\theta\cos\omega t - A(t)\sin\theta\sin\omega t \qquad (1)$$

State variables at time t_k are defined as:

$$X1_k = A(t_k)\cos(\omega t_k + \theta) \qquad (2)$$

$$X2_k = A(t_k)\sin(\omega t_k + \theta) \qquad (3)$$

[Downloaded from jiaeee.com on 2026-11-20]

To write the state equations let us consider the signal at time t_{k+1}:

$$X1_{k+1} = A(t_{k+1})\cos(\omega t_k + \omega\Delta t + \theta) = X1_k \cos(\omega\Delta t) - X2_k \sin(\omega\Delta t) \quad (4)$$

and for second state variable $X2_{k+1}$:

$$X2_{k+1} = A(t_{k+1})\sin(\omega t_k + \omega\Delta t + \theta) = X1_k \sin(\omega\Delta t) + X2_k \cos(\omega\Delta t) \quad (5)$$

From (4) and (5), the state variable equations will be:

$$\begin{bmatrix} X1 \\ X2 \end{bmatrix}_{k+1} = \begin{bmatrix} \cos(\omega\Delta t) & -\sin(\omega\Delta t) \\ \sin(\omega\Delta t) & \cos(\omega\Delta t) \end{bmatrix} \begin{bmatrix} X1 \\ X2 \end{bmatrix}_k + \begin{bmatrix} w_1 \\ w_2 \end{bmatrix}_k \quad (6)$$

In equation (6), the time variations of state variables are described by random variables w_1 and w_2. Measurement is made at time t_k according to the relation given by the equation:

$$Z_k = \begin{bmatrix} 1 & 0 \end{bmatrix} \begin{bmatrix} X1 \\ X2 \end{bmatrix}_k + v_k \quad (7)$$

where the scalar v_k represents the measurement noise and its variance will be denoted by R_k. Now, considering a signal with n different frequencies as:

$$s(t) = \sum_{i=1}^{n} A^{(i)}(t)\cos(i\omega t + \theta^{(i)}) \quad (8)$$

By selecting 2n state variables as:

$$X1_k^{(i)} = A^{(i)}(t_k)\cos(i\omega t_k + \theta^{(i)}) \quad (9)$$

$$X2_k^{(i)} = A^{(i)}(t_k)\sin(i\omega t_k + \theta^{(i)}) \quad (10)$$

the state equations can be presented in matrix form:

$$\begin{bmatrix} X1^{(1)} \\ X2^{(1)} \\ \vdots \\ X1^{(n)} \\ X2^{(n)} \end{bmatrix}_{k+1} = \begin{bmatrix} M^{(1)} & 0 & 0 & 0 & 0 \\ 0 & \ddots & & \iddots & 0 \\ 0 & & \ddots & & 0 \\ 0 & \iddots & & \ddots & 0 \\ 0 & 0 & 0 & 0 & M^{(n)} \end{bmatrix} \begin{bmatrix} X1^{(1)} \\ X2^{(1)} \\ \vdots \\ X1^{(n)} \\ X2^{(n)} \end{bmatrix}_k + \begin{bmatrix} w_1^{(1)} \\ w_2^{(1)} \\ \vdots \\ w_1^{(n)} \\ w_2^{(n)} \end{bmatrix}_k \quad (11)$$

The submatrices $M^{(i)}$ are similar to:

$$M^{(i)} = \begin{bmatrix} \cos(i\omega\Delta t) & -\sin(i\omega\Delta t) \\ \sin(i\omega\Delta t) & \cos(i\omega\Delta t) \end{bmatrix} \quad (12)$$

The measurement equation then will be

$$Z_k = \begin{bmatrix} 1 & 0 & \cdots & 1 & 0 \end{bmatrix} \begin{bmatrix} X1^{(1)} \\ X2^{(1)} \\ \vdots \\ X1^{(n)} \\ X2^{(n)} \end{bmatrix}_k + v_k \quad (13)$$

With this selection of state variables, the amplitude and phase angle of each harmonic can be computed by:

$$A^{(i)} = \sqrt{\left(X1^{(i)}\right)^2 + \left(X2^{(i)}\right)^2} \quad (14)$$

$$\theta^{(i)} = \tan^{-1}\left(\frac{X2^{(i)}}{X1^{(i)}}\right) \quad (15)$$

The above calculations impose increased computational burden due to the special form of state variables selection. However, the form of state variables is quite useful for computing the frequency needed for the auto- synchronization algorithm described later. In addition, with this selection of state variables, the components of the Kalman gain vector become constants and can be computed off-line. The recursive KFA is shown in Fig. 1. In this figure, Q_k represents the covariance matrix of the process noise vector $\widehat{w}_k$. The state transition matrix ϕ_k and the constant matrix H_k are the coefficient matrices in equations (11) and (13), respectively.

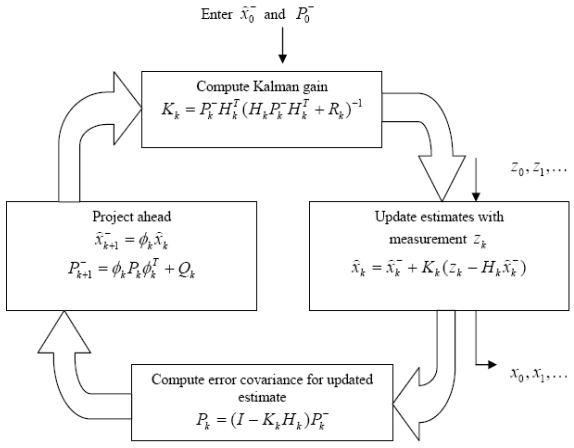


Fig. 1: Kalman Filter Algorithm

3. Auto-Synchronization Algorithm

In order to eliminate the errors occurred due to variations in the incoming signal frequency, we decided to use the output of the Kalman filter to estimate the actual frequency of the incoming signal. This idea was initiated when it was realized,

[Downloaded from jiaeee.com on 2026-11-20]

following numerous simulations, that even though there were errors in the estimated fundamental frequency state variables, however the frequency of these variables well followed the variations in the frequency of the incoming signal. Thus, to estimate the frequency, the instantaneous frequencies of the fundamental frequency state variables were averaged over five cycles with the instantaneous frequency being proportional to the ratio of the derivative of in-phase fundamental frequency component to the quadrature-phase fundamental frequency component.

Now, the KFA could be synchronized by updating the Kalman filter equations using the estimated frequency having in mind that both the Kalman gain and the state transition matrices are functions of fundamental frequency. The gain matrix is computed off-line thus, updating it with the estimated frequency makes the entire algorithm very slow and useless for our purposes. Fortunately, it was discovered that if only the transition matrix were updated using the estimated frequency and the gain matrix were computed at the fundamental 50 Hz frequency, the results would be completely satisfactory. Thus, the KFA auto-synchronization was done by just updating the state transition matrix.

4. Simulation Results

In this section, the performance and efficiency of the KFA is studied by means of simulations implemented in MATLAB. The Kalman filter parameters were selected as bellow:

R = Measurement noise variance was selected to be constant (0.05 $p.u.^2$);

Q = Process noise covariance matrix (a diagonal matrix with diagonal elements equal to 0.05 $p.u.^2$);

$\hat{x}_0^-$ = Initial state vector (a zero vector);

P_0^- = Initial error covariance matrix (a diagonal matrix with diagonal elements equal to 10 $p.u.^2$);

f_c = Power system fundamental frequency (50 Hz) and

f_s = Sampling frequency (3200 Hz).

In order to study the ability of the algorithm in tracking time-varying harmonics, a sample test signal of the form:

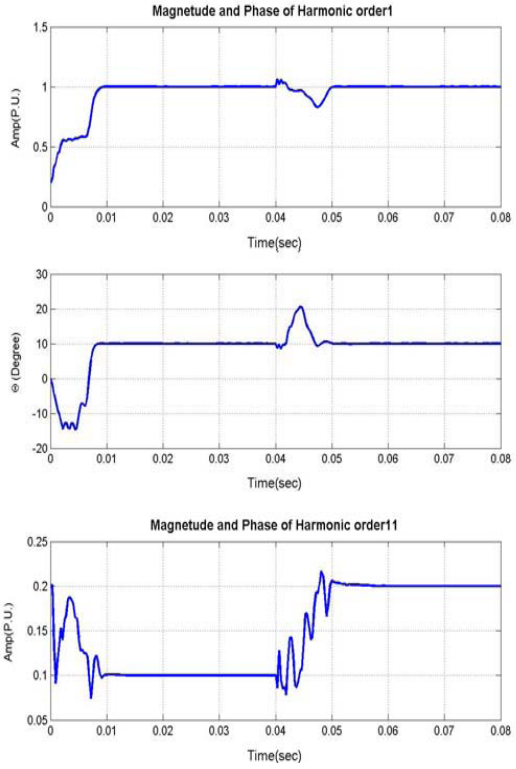
$$s(t)=\begin{cases} s_1(t) & 0<t<0.04 \quad s \\ s_2(t) & 0.04<t<0.12 \quad s \end{cases} \qquad (16)$$

$$s_1(t)=\cos(\omega t+10^\circ)+0.3\cos(3\omega t+20^\circ)+0.1\cos(11\omega t+30^\circ)+0.05\cos(19\omega t+40^\circ) \qquad (17)$$

$$s_2(t)=\cos(\omega t+10^\circ)+0.8\cos(3\omega t+20^\circ)+0.2\cos(11\omega t+30^\circ)+0.1\cos(19\omega t+40^\circ) \qquad (18)$$

is considered. Amplitude and phase angle estimated by the KFA simulation are shown in Fig 2. There is a convergence period at the start of estimation that lasts about 10 ms depending on the initial values selected for recursive algorithm. Several studies showed that the length of this convergence period is constant when the equations are written for 50 Hertz system. Fortunately, this transient period only appears at the algorithm starting section and is referred to as the initiation period.

Another noticeable fact seen in Fig. 2 and confirmed by the results of numerous simulations performed is that the KFA has a delay in responding to sudden changes in the signals. This delay is an unavoidable characteristic of KFA. The delay period is about 10 ms and it depends on the fundamental frequency and the process noise matrix Q. Although this delay decreases when Q increases, however it will lose one important factor of the KFA which is the noise rejection property. Therefore, the KFA has a limited speed for tracking very fast changing harmonics.



[Downloaded from jiaeee.com on 2026-11-20]

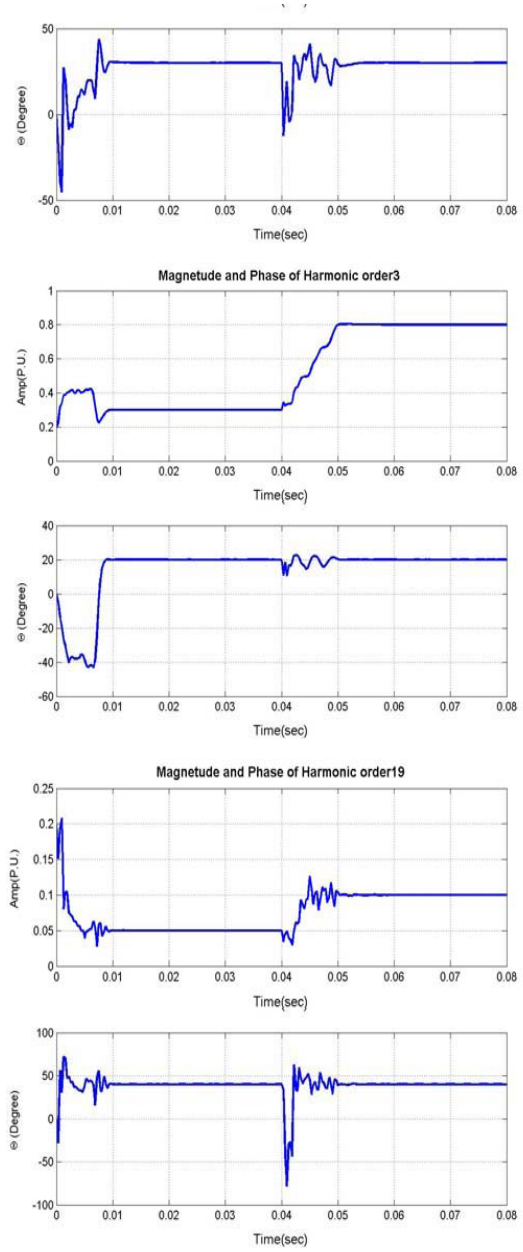


Fig. 2: Step response of Kalman filter in amplitude estimation of harmonic orders 1, 3, 11 and 19

In order to study the algorithm ability for tracking continuous variations in harmonics, the following test signal is applied:

$$s(t) = B(t) \times s_1(t) \tag{19}$$

$$s_1(t) = \cos(\omega t) + 0.1\cos(3\omega t + 10^{\circ}) + 0.1\cos(5\omega t + 20^{\circ}) + 0.08\cos(7\omega t + 30^{\circ}) + 0.08\cos(11\omega t + 40^{\circ}) + 0.05\cos(13\omega t + 50^{\circ}) + 0.05\cos(19\omega t + 60^{\circ}) \tag{20}$$

$$B(t) = \begin{cases} 1 & 0 < t < 0.2 \ \ s \\ 1 + 5(t - 0.2) & 0.2 < t < 0.4 \ \ s \\ 2 & 0.4 < t < 0.6 \ \ s \\ 2 - 5(t - 0.6) & 0.6 < t < 0.8 \ \ s \\ 1 & 0.8 < t < 1 \ \ s \end{cases} \tag{21}$$

This signal is shown in Fig. 3 and as seen in Fig. 4, the continuous variations are well followed by the KFA.

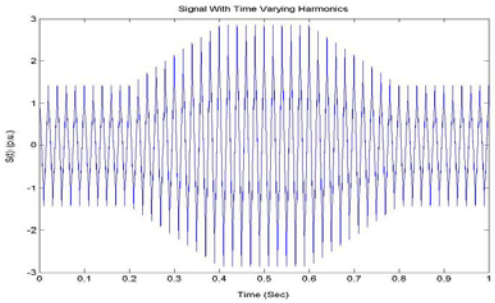


Fig. 3: Test signal wave shape

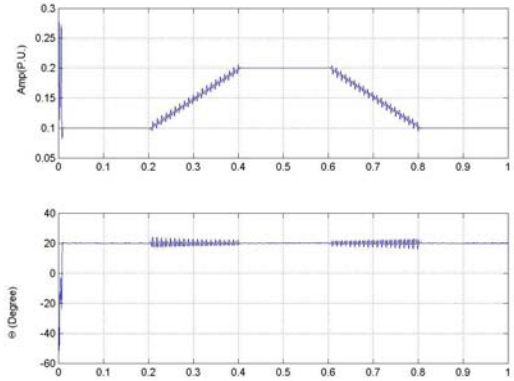


Fig. 4: Amplitude and phase angle of the 5th harmonic

5. Practical Results

Based on the KFA described, a prototype harmonic analyzer was designed and constructed. The analyzer has two input ports; one for signals having peaks of 5 volts and less used for testing and calibrating the analyzer and another input port for signals having peaks of 600 volts maximum. The prototype device consists of a hardware and a software modules. The hardware module includes anti-aliasing filter, input buffer and surge/overvoltage protector, sample and hold and A/D converter, main and microcontroller power supplies, RS232 converter and output opto-isolator. Data sampling followed by data transferring

[Downloaded from jiaeee.com on 2026-11-20]

to a personal computer serial port is performed by the microcontroller-based hardware module in real-time. Then, the software module running on a PC, performs the KFA to estimate the individual harmonic distortions (IHD's) and THD of the incoming signal online.

In order to analyze the performance of the fabricated prototype analyzer, several distorted signals with different known characteristics were generated in MATLAB and exported in analogue format from PC sound card. These signals then were applied as inputs to the hardware module. As an example, the following signal is considered:

$$s(t) = \begin{cases} s_1(t) & t < 12.3 \ \ s \\ s_2(t) & t > 12.3 \ \ s \end{cases} \qquad (22)$$

$$s_1(t) = \cos(\omega t) + 0.3\cos(3\omega t) + 0.2\cos(7\omega t) \qquad (23)$$

$$s_2(t) = \cos(\omega t) + 0.4\cos(3\omega t) + 0.3\cos(7\omega t) \qquad (24)$$

The third harmonic amplitude of the above signal estimated by the prototype analyzer is shown in Fig. 5. The algorithm could identify the correct amplitude in less than one-half the fundamental cycle.

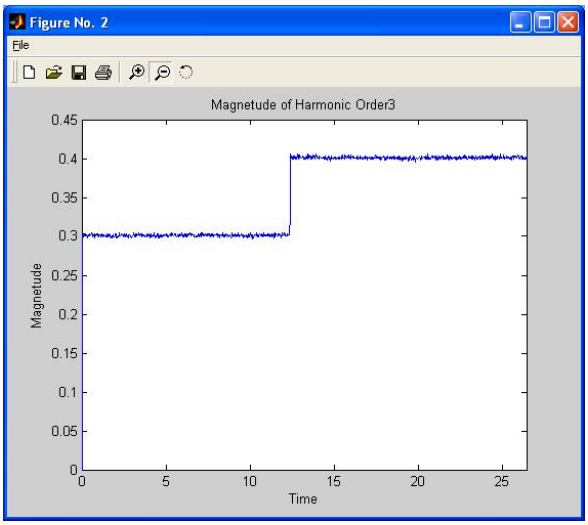


Fig. 5: Third harmonic measured by analyzer

Figure 6 shows the results of a real-time measurement made by the prototype analyzer at a factory nearby a 6-pulse rectifier. Table 1 shows harmonics amplitudes of the same signal that were measured by a commercial harmonic analyzer (LEM Analyst 2060). The differences in the two measurements related to the 2nd, 29th and 31st harmonics are due to the 1% measurement error caused by the microcontroller (ATmega32) built-in 10-bit A/D converter.

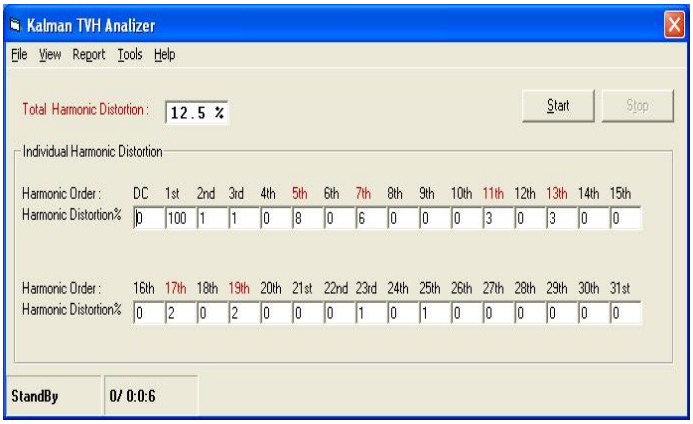


Fig. 6: Practical measurement from utility main voltage

Table 1: Harmonic amplitude which measured by a commercial harmonic analyzer

Harmonic Order	1	2	3	4	5	6	7	8	9	10	11	12	13	14	15	16
Amplitude (%)	100	0	1	0	8	0	6	0	0	0	3	0	3	0	0	0
Harmonic Order	17	18	19	20	21	22	23	24	25	26	27	28	29	30	31	
Amplitude (%)	2	0	2	0	0	0	1	0	1	0	0	0	1	0	1	

6. Cumulative Harmonic Curves

After accurate on-line measurement of time-varying harmonics and total harmonic distortion, it is necessary to employ a statistical approach, because of the variable nature of distortion level, in order to evaluate the severity of time-varying harmonics. Most standards consider harmonics as steady state phenomena. Therefore, the limitations set by those standards for the harmonic components and THD cannot be used directly for the time-varying harmonics cases. To solve this problem in a way that the steady state harmonics limits could be applied to the time-varying harmonics and also to present a way to handle short time excursions above steady state harmonics limits [17], cumulative time curves were introduced.

For FFT-based instruments, IEC standard 61000-4-7 [18] recommends three window widths for different categories of harmonics. Moreover, this standard recommends five time intervals for the purpose of data compressions. These recommendations lead to what the IEC standard calls it "cumulative probability function (probability of not exceeding the corresponding value)". We extended this idea to the KFA output having in mind that the gaps between the window times and between time intervals are of no concern with regards to KFA since the KFA estimates harmonic components continuously in real-time. In addition, the low

[Downloaded from jiaeee.com on 2026-11-20]

computational requirements needed by the Kalman method make it possible to obtain cumulative severity factors on-line giving more information about the distortion severity that the IEC standard method gives.

The prototype harmonic analyzer performs data sampling at 3200 Hz. For each sample, THD and harmonics content up to the 31st harmonic are estimated in real-time. Every 64 consecutive THD and individual harmonic distortions values are averaged and the results are kept temporarily. These averaged values are used for computing the cumulative times explained later.

The user defines three thresholds for THD and three thresholds for each IHD. These thresholds could be (and better be) different for different IHD's. We suggest the first set of THD and individual harmonic thresholds to be the maximum allowed steady state THD and individual harmonic distortions limits and the second and the third sets of thresholds to be twice and three times of the first set, respectively. The user also defines three cumulative time percentage thresholds corresponding to the three distortion threshold sets. We suggest 5%, 1% and 0.1% time thresholds for the first, second and third sets of distortion thresholds, respectively.

Every one second, temporarily kept THD and individual harmonic distortions values are averaged and the results are displayed on the monitor and stored on the hard disk. In addition, every one second, the cumulative times, as percentage of the total measurement period, of occurrence of THD and each IHD that exceed the defined distortion thresholds are computed, displayed and compared against the defined cumulative time percentage thresholds. Whenever any of the on-line computed cumulative times, referred to as cumulative time indices (factors), related to THD or any of the IHD's exceeds the time thresholds, the color of numbers showing the cumulative times will change from black to red. By this, we allow the cumulative times of occurrence of harmonics severer than the steady state limits, severer than twice the steady state limits and three times the steady state limits to be at most 5%, 1% and 0.1% of the total measurement period, respectively.

The cumulative curves can be plotted in off-line mode for any user specified time duration of the total measurement period. For each THD level on the horizontal axis, the cumulative time of occurrence of THD values exceeding that particular level is computed as percentage of the time duration specified by the user, to plot a curve similar to that shown in Fig. 7. On this curve, the distortion and time thresholds are shown as three steps. An acceptable harmonic distortion is the one for which its cumulative time curve lies under the three-step limit. Similar cumulative curves can be plotted for any individual harmonic distortions.

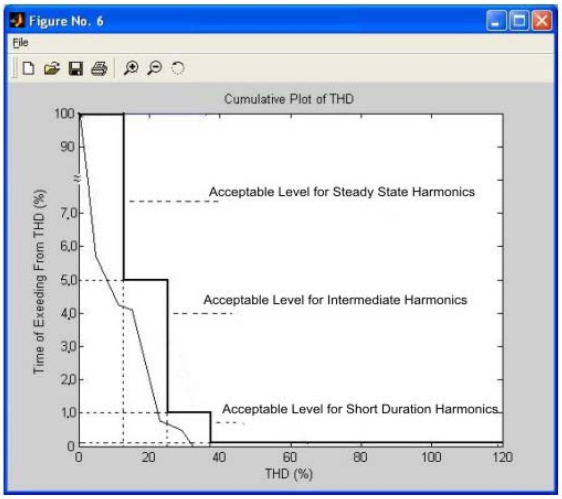


Fig. 7: Cumulative harmonic distortion curve with its acceptance levels

7. CONCLUSIONS

The need for having a device capable of online measuring, monitoring and assessing time-varying harmonics, motivated us to design and fabricate a prototype Kalman filter-based harmonic analyzer. Against drawbacks of Fourier transform-based methods for harmonics measurement, specially in the present of time-varying harmonics, Kalman filter algorithm has outstanding advantages including good noise rejection property, ability to obtain desired frequency resolution independent of time resolution, not requiring synchronized sampling, low computational requirements, ability to track time-varying harmonics and ability to perform on-line measurements.

A powerful software module accompanies the microcontroller-based hardware module. An auto-synchronization algorithm for estimating the frequency of the incoming signal, estimating and reporting THD and individual harmonic distortions levels and also providing cumulative times of occurrence of THD and all IHD's exceeding user defined thresholds (three thresholds for THD and three thresholds for each IHD) are on-line capabilities of the device.

We proposed cumulative time curves for THD and all IHD's as means for evaluating the severity of time-varying harmonics and as criteria for judging whether the harmonic pollution is acceptable. These

[Downloaded from jiaeee.com on 2026-11-20]

curves are plotted in off-line mode depicting, for any THD level among the entire range of THD shown on the horizontal axis, the cumulative time of occurrence of THD's that exceed that particular level of THD as the percentage of total monitoring time. Similar cumulative time cures can be plotted for each IHD. We allowed the cumulative times of occurrence of distortions severer that the steady state harmonics limits, twice the steady state harmonics limits and three times the steady state harmonics limits to be at most 10%, 1% and 0.1% of the total monitoring time. These acceptance criteria appear as three steps and harmonic pollutions corresponding to the curves underlying these steps are accepted. The harmonic and time thresholds presented in this paper are the authors preferences. These thresholds can be defined by the use to be in agreement with any national or international standard. Indeed, the idea of cumulative time curves is strong enough to be used by international committees as a base for establishing time-varying harmonics assessment procedures

REFERENCES

[1] Lazendby, H., and Zivanovic, R., "Some Observations on the Time-varying Harmonics and Inter Harmonics", IEEE Transactions on Power Delivery, pp. 849-852, 1999.

[2] Hlawatsch, F. and Boudraux-Bartels, G.F., "Linear and Quadratic Time-Frequency Signal Representation", IEEE Signal Processing Magazine, pp. 21-76, April 1992.

[3] Poisson, O., Rioval, P., and Meunier, M., "New Signal Processing Tools Applied to Power Quality Analysis", IEEE Transactions on Power Delivery, pp. 561-566, April 1999.

[4] Van den Keybus, J., Driesen, J., and Belmans, R., "Using Fourier Transform and Model Based Filters to Measure Time-Varying Harmonics", Proceedings of the IEEE Power Engineering Society General Meeting, Vol. 3, pp 2402-2406, June 2005.

[5] Miegeville, L. and Guerin, P., "Identification of Time-Varying Pattern of Periodic Harmonics", IEEE Transactions on Power Delivery, pp. 845-852, April 2006.

[6] Moo, C.S., Chang, N.Y., and Mok, P.P., "A Digital Measurement Scheme for Time-varying Transient Harmonics", IEEE Transactions on Power Delivery, pp. 588-594, April 1995.

[7] Heydt, G. T., Liu, C. C., and Tu, L., "Application of the Windowed FFT to Electric Power Quality Assessment", IEEE Transactions on Power Delivery, pp. 1411-1416, October 1999.

[8] Heydt, G. T., and Gewell, W. T., "Pitfalls of Electric Power Quality Indices", IEEE Transactions on Power Delivery, pp. 570-577, April 1998.

[9] Lin, H. C., "Fast Tracking of Time-Varying Power System Frequency and Harmonics Using Iterative-Loop Approaching Algorithm", IEEE Transactions on Industrial Electronics, pp 974-982, April 2007.

[10] Liew, A. C., "An Adaptive Linear Combiner for Online Tracking of Power System Harmonics", IEEE Transactions on Power Systems, pp. 1730-1736, Nov. 1996.

[11] Lai, L. L., Chen, W. L., Tse, C. T., and So, A. T. P., "Real-Time Frequency and Harmonic Evaluation Using Artificial Neural Networks", IEEE Transactions on Power Delivery, pp. 52-59, Jan. 1999.

[12] Wang, J., and Ran, Q., "Time-Varying Transient Harmonics Measurement Based on Wavelet Transform", Proceedings of the IEEE Instrumentation and Measurement Technology Conference, pp. 1556-1559, June 1996.

[13] Lin, T., and Yamada, E., "Wavelet Approach to Power Quality Monitoring", Proceedings of the IEEE Industrial Electronics Society Annual Conference, pp. 670-675, 2001.

[14] Brown, R.G., and Hwang, Y.C., Introduction to Random Signal and Applied Kalman Filtering, Third Edition, John Willy and Sons, 1996.

[15] Adly, A., Girgis, W., Chang, B., and Makram, E., "A Digital Recursive Measurement Scheme for On-line Tracking of Power System Harmonics", IEEE Transactions on Power Delivery, pp. 1153-1160, July 1991.

[16] Kennedy, K., Lightbody, G., and Yacamini, R., "Power System Harmonic Analysis Using the Kalman Filter", Proceedings of the IEEE Power Engineering Society General Meeting, Vol. 1, pp. 752-757, July 2003.

[17] Ortmeyer, T., Xu, W., "Setting Limits on Time Varying Harmonics", Proceedings of the IEEE Power Engineering Society General Meeting, Vol. 2, pp 1172-1175, July 2003.

[18] IEC Standard 1000-4-7, Electromagnetic Compatibility (EMC), Part 4. Testing and Measurement Techniques, Section 7. General Guide on Harmonics and Interharmonics Measurements and instrumentation for Power Supply Systems and Equipment Connected Thereto", 1991.

[Downloaded from jiaeee.com on 2026-11-20]